

On the difference between breakdown and quench voltages of argon plasma and its relation to $4p - 4s$ atomic state transitions

Ebrahim Forati,^{*} Shiva Piltan, and Dan Sievenpiper[†]

University of California San Diego

(Dated: December 18, 2014)

Using a relaxation oscillator circuit, breakdown (V_{BD}) and quench (V_Q) voltages of a DC discharge microplasma between two needle probes are measured. High resolution modified Paschen curves are obtained for argon microplasmas including a quench voltage curve representing the voltage at which the plasma turns off. It is shown that, for a point to point microgap (e.g. the microgap between two needle probes) which describes many realistic microdevices, neither Paschen's law applies nor field emission is noticeable. Although normally $V_{BD} > V_Q$, it is observed that depending on environmental parameters of argon, such as pressure and the driving circuitry, plasma can exist in a different state with equal V_{BD} and V_Q . Using emission line spectroscopy, it is shown that V_{BD} and V_Q are equal if the atomic excitation by the electric field dipole moment dominantly leads to one of the argon's metastable states ($4P_5$ in our study).

Microplasma, which typically refers to a cold (non-thermal) plasma confined to sub-millimeter dimensions, began to appear in the literature in the mid 1990s. Besides numerous biological and environmental applications, microplasmas are also being used for gas and surface analysis, and in ultraviolet radiation sources [1–4]. In a DC discharge plasma, the electron impact on gas atoms or molecules and the secondary electron emission are the two main processes to sustain the plasma. Such processes are mostly dependent on the gas characteristics (e.g. pressure and temperature), the electrodes' conditions (e.g. material, surface finish, shape, area, and separation), and the driving circuitry [5–9]. Based on the Townsend's theorem, the breakdown criterion for a DC discharge plasma in a 1-D geometry can be expressed as

$$\gamma (e^{\alpha d} - 1) = 1, \quad (1)$$

in which α , also known as Townsend's first coefficient, is the number of ionizing collisions made by one electron per unit distance and γ , also known as Townsend's second coefficient, is the number of secondary electrons produced at the cathode per ionizing collision in the gap. Assuming that electrons move through a uniform electric field ($E = V/d$) and gas pressure (p), their mean energies will be proportional to the ratio $V/(pd)$, where V and d are voltage and gap size, respectively. The breakdown voltage is then expected to depend on (pd) , generally known as Paschen's law as

$$V_{BD} = \frac{Bpd}{\ln(pd) + \ln(A/\ln(1/\gamma + 1))}, \quad (2)$$

where A and B are gas related constants mostly obtained experimentally. The Townsend's theorem leads to the well-known traditional Paschen curves for breakdown voltage as a function of (pd) with a minimum and two upturn arms (approximately V-shaped) [10, 11]. For

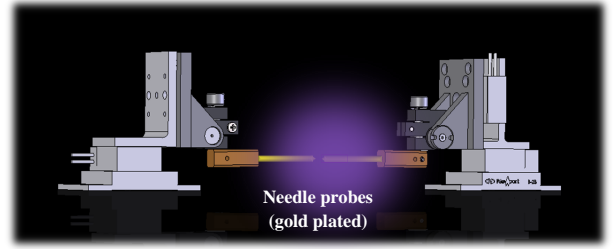


FIG. 1: The point-point microgap between two needle probes igniting an argon microplasma. The probe holders are mounted on nano-positioners for xyz adjustments and the entire geometry is fitted inside the box chamber shown in Fig. 2.

a fixed gap size on the right arm of the Paschen curve, pressure and V_{BD} are proportional because of the increase of collisions between electrons and ions/atoms preventing electrons from gaining adequate kinetic energy for gas ionization. On the left arm of the Paschen curve, pressure and V_{BD} are inversely proportional due to the decrease in the number of species contributing to cascade ionization [12–14].

It is suggested by researchers at Bell Laboratories that the electron field emission becomes more significant in small gap sizes at some point. Below $5\mu\text{m}$ in atmospheric pressure, it becomes the dominant process sustaining the plasma. Electron field emission, also called Fowler-Nordheim tunneling, is the process whereby electrons tunnel through a potential barrier (e.g. a metal surface) in the presence of a high electric field [15–21] (this is different from thermionic emission in which electrons emit over the barrier due to the high temperature [22]). The Fowler-Nordheim equation describes the electron field emission current (I) as [23, 24]

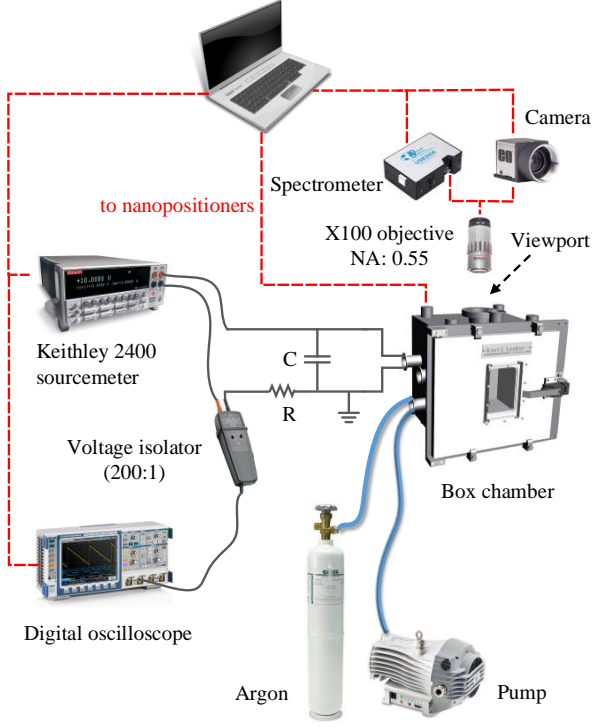


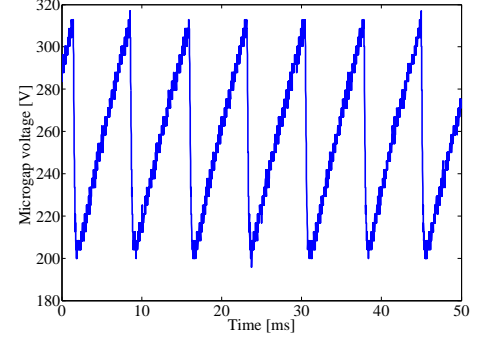
FIG. 2: The measurement setup.

$$I = aE^2 \exp\left(\frac{-b\Phi^{1.5}}{E}\right), \quad (3)$$

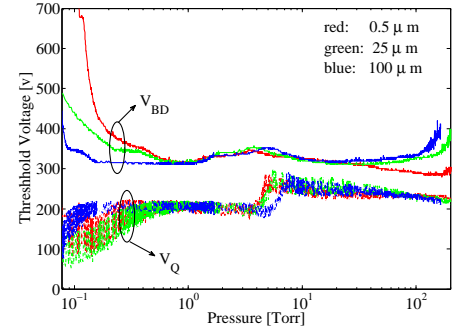
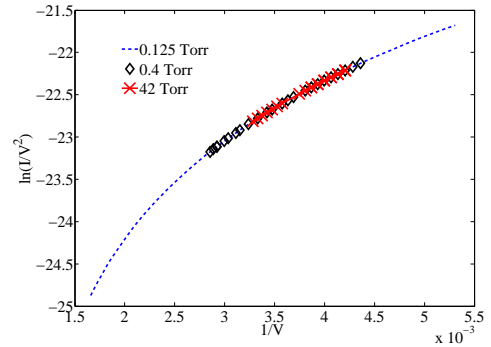
where a and b are constants, E is the electric field and Φ is the work function associated with the material of the electrodes.

For microplasmas with small gap sizes, combination of Townsend and Fowler-Nordheim theorems leads to a modified Paschen curve, as shown in Ref. [10]. The modified paschen curve replaces the left upturn of the pure Paschen curve with a plateau and a decline to zero [25, 26]. Nevertheless, both traditional and modified Paschen curves are derived based on 1-D geometries and are confirmed experimentally to be accurate for electrodes much larger than the gap size [27–35]. However, in a practical microplasma device, the size of the electrodes has to be comparable to the gap size to retain all of the device dimensions in the sub-millimeter range [36, 37]. Along with an ongoing effort to design practical microplasma devices, here we study argon microplasma properties in a point-point geometry, i.e. between two gold plated needle probes with tip diameter $10\ \mu\text{m}$ and length 5 cm , as shown in Fig. 1. The probe holders are mounted on three nano-positioners for xyz adjustments with an accuracy 50 nm .

Although a DC discharge plasma ignites at V_{BD} , it can normally be sustained with lower applied voltages since



(a) Measured sawtooth across the 500 nm microgap at 0.9 Torr,

(b) Measured V_{BD} and V_{Q} of the argon microplasma with different gap sizes,

(c) Fowler-Nordheim plot of 500 nm gap size at different pressures,

FIG. 3: Measured argon microplasma results.

the rise of its free electrons' temperature and number helps the ionization processes. In other words, usually the DC breakdown voltage of a plasma is higher than its quench voltage (V_{Q}), in which the plasma turns off, leading to a hysteresis property for the plasma. Depending on the application, the quench voltage of a plasma may become a critical parameter as important as the breakdown voltage (e.g. in switching applications). Despite

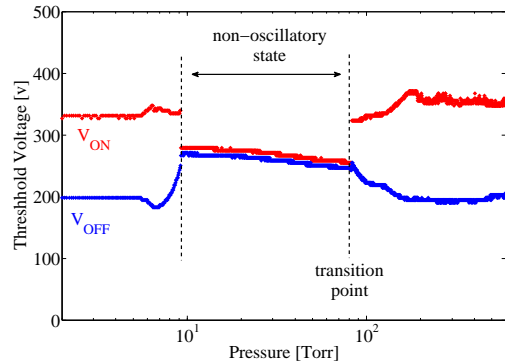
extensive studies on DC breakdown voltage, we are not aware of any investigations concerning the quench voltage of plasmas. Here, by inserting the point-point microplasma of Fig.1 (with variable pressure and gap size) into a relaxation oscillator circuit [38, 39], we measure its breakdown and quench voltages accurately. The measurement setup, including the relaxation oscillator circuit, is shown in Fig. 2, in which the sourcemeter provides DC voltage. It is quite easy to show that due to the difference between V_{BD} and V_Q of the plasma, a sawtooth voltage appears across the microplasma with the frequency

$$f = \frac{1}{R_{\text{total}}C} \ln \left(\frac{V_{DC} - V_{BD}}{V_{DC} - V_Q} \right) \quad (4)$$

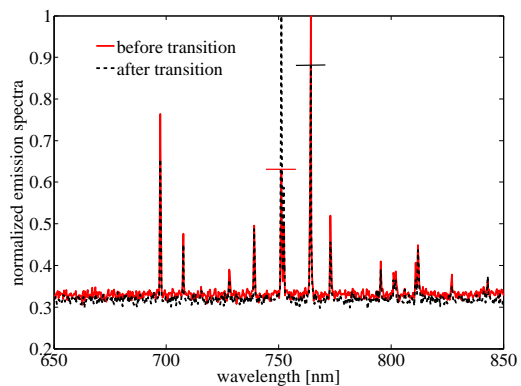
in which V_{DC} is the applied DC voltage and C is the parallel capacitor. The input resistance of the voltage isolator is $2\text{ M}\Omega$ and $R_{\text{total}} = R + 2\text{ M}\Omega$ is the total series resistance. As an example, Fig. 3(a) shows the measured sawtooth voltage for $V_{DC} = 700\text{ V}$, $C = 60\text{ pF}$, and $R_{\text{total}} = 52\text{ M}\Omega$. The argon microplasma pressure (p) and gap size (d) are 0.9 Torr and 500 nm , respectively.

The extremums of the sawtooth are essentially V_{BD} and V_Q of the microplasma. Besides repeatability, this relaxation oscillator technique enables us to extract statistical information about V_{BD} and V_Q (such as average and standard deviation) simply by reading enough periods of the sawtooth. Moreover, the current versus voltage ($I - V$) information of the microplasma can be obtained easily by sampling enough points during the breakdown to quench transition (i.e. the sharp transition in the sawtooth). Using this strategy, it will be shown that field emission is not significant in the point-point geometry even with small gap sizes.

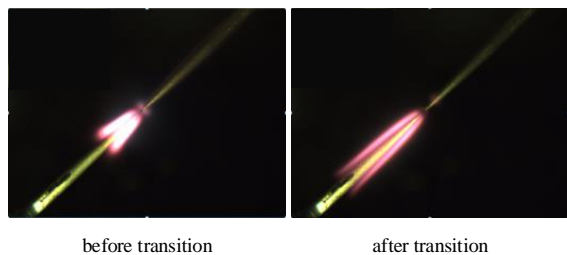
Figure 3(b) shows V_{BD} and V_Q of the argon microplasma as a function of pressure for three different gap sizes including a very small (500 nm) gap size which does not follow Paschen's law (neither traditional nor modified versions including electron field emission effect). The relaxation oscillator parameters used to generate Fig. 3 are $V_{DC} = 900\text{ V}$, $R = 50\text{ M}\Omega$, and $C = 60\text{ pF}$. The Paschen's law's failure to explain point-point geometries is a result of the fact that Townsend's theorem is based on a 1-D geometry (i.e. an infinite plane-plane geometry). Nonetheless, Paschen's law has been observed [10, 34, 35] to be an acceptable approximation for line-line geometries (i.e. the gap between edges of two coplanar rectangles). In the point-point geometry, different path lengths exist between the two probes where the smallest path length is equal to the gap size. The measured Paschen curve is then the minimum envelope of all possible traditional Paschen curves between the two needles. On the other hand, the field emission contribution in Fig. 3(b) is negligible because only a small area of each probe (i.e. the tips of the probe) is exposed to intense electric field. In order to confirm this, curves of $\ln(I/V^2)$ versus $1/V$ of the gap size $0.5\text{ }\mu\text{m}$ and at several pressures



(a) V_{BD} and V_Q for gap size $64\text{ }\mu\text{m}$, $R = 2\text{ M}\Omega$, $C = 60\text{ pF}$, and $V_{DC} = 800\text{ V}$,



(b) Emission spectra before and after transition from non-oscillatory to oscillatory state,



(c) Glow pattern of non-oscillatory (left) and oscillatory (right) states,

FIG. 4: Oscillatory and non-oscillatory states of argon plasma.

are extracted from the sawtooth waveform and shown in Fig. 3(c). This plot, also known as Fowler-Nordheim plot, clarifies if Equation (3) (and therefore field emission) governs the process. The fact that the curves in Fig. 3(c) are not straight lines with negative slopes, as Equation (3) predicts, proves that electron field emission is negligible.

It is evident from Fig. 3(b) that both V_{BD} and V_Q are almost independent of the gap size and identically depend on the pressure. In fact, several other gap sizes have been measured in the range $0.5 - 1000 \mu m$ and they all have similar trends. The breakdown voltage has a local peak at 3 Torr, and the quench voltage has minimum difference from the breakdown voltage at around 5 Torr.

Depending on the plasma parameters such as pressure and the driving circuitry, electron impact and the electric field dipole moment (by the applied voltage) can force argon atoms to the excited states with different probabilities (even zero) of return to the ground state. These different probabilities relate to the difference between V_{BD} and V_Q . There are combinations of plasma parameters in which V_{BD} can become equal to V_Q . For instance, Fig. 4 shows V_Q and V_{BD} of the point-point microplasma (with gap size $64 \mu m$, $V_{DC} = 800 V$, and $R = 0 M\Omega$) with two distinct plasma states: one with $V_Q \neq V_{BD}$ is called the oscillatory state (since it can generate the sawtooth), and the other a non-oscillatory state with $V_{BD} = V_Q$ (incapable of producing the sawtooth). Normalized emission spectra [40, 41] and glow patterns of the two states are shown in Figs. 4(b) and 4(c) just before and after the states transition from non-oscillatory to oscillatory behavior as indicated in Fig. 4(a). The argon emission line at $\lambda = 763.5 nm$, dominant in the non-oscillatory plasma state, indicates the $1S_5 - 2P_6$ argon atomic state transition (in Paschen's notation), and the argon emission line at $\lambda = 751.5 nm$, dominant in the oscillatory plasma mode, relates to the $1S_4 - 2P_5$ argon atomic state's transition [42–44]. However, there is a fundamental difference between the final states of the two transitions (which are $2P_6$ and $2P_5$ states) explaining the difference between the two plasma states. The atomic state $2P_5$ is a metastable state, meaning quantum mechanical laws forbid any electron transition from $2P_5$ to the ground state. But, the atomic state $2P_6$ is a resonant state with allowed transition to the ground state. As Fig. 4(c) shows, most of the electron transitions in the oscillatory state of the argon plasma lead to a metastable state where they will be trapped at a high energy level (11.65 eV higher than the ground state, while the ionization energy of argon is 15.76 eV [45]) for a relatively long time (the life time is 56 s for $2P_5$ state). As a result, electrons with lower kinetic energy have the chance to ionize these metastable atoms leading to a lower V_Q than V_{BD} . In other words, as soon as the metastable atoms are generated after the plasma ignition, lower applied voltages (leading to electrons with lower kinetic energy) can sustain the plasma. On the contrary, in the non-oscillatory mode of the plasma, the outer shell electrons of most of the argon atoms experience a step transition from $1S_5$ to the ground state (through $2P_6$) leading to lower population of metastable atoms (and therefore equal V_Q and V_{BD}).

In summary, we have introduced an easy and practical

way to measure both V_{BD} and V_Q of DC discharge plasmas. Aside from the breakdown voltage, we have studied the quench voltage of microplasmas for the first time. We also have shown that Townsend and Fowler-Nordheim theorems cannot be used in the form of traditional or modified Paschen curves to predict the breakdown voltage of point-point microplasmas. More importantly, we have shown that depending on the number density of the argon metastable atoms, two different states of plasma, with and without equal V_{BD} and V_Q , can exist.

* forati@ieee.org

† dsievenpiper@ucsd.edu

- [1] R. Foest, M. Schmidt, and K. Becker, *International Journal of Mass Spectrometry* **248**, 87 (2006).
- [2] A. Papadakis, S. Rossides, and A. Metaxas, *Open Applied Physics Journal* **4**, 45 (2011).
- [3] Y. Li and D. B. Go, in *International Workshop on Microplasmas, Paris, France* (2011).
- [4] K. H. Becker, U. Kogelschatz, K. Schoenbach, and R. Barker, *Non-equilibrium air plasmas at atmospheric pressure* (CRC press, 2004).
- [5] N. S. J. Braithwaite, *Plasma sources science and technology* **9**, 517 (2000).
- [6] Y. P. Raizer, V. I. Kisin, and J. E. Allen, *Gas discharge physics*, Vol. 1 (Springer-Verlag Berlin, 1991).
- [7] K. Yanallah, F. Pontiga, and A. Castellanos, *Journal of Physics D: Applied Physics* **44**, 055201 (2011).
- [8] N. Kopeika, B. Galore, D. Stempler, and Y. Heimenrath, *Microwave Theory and Techniques, IEEE Transactions on* **23**, 843 (1975).
- [9] T. Iwao, H. Miyazaki, and T. Inaba, *Vacuum* **73**, 359 (2004).
- [10] D. B. Go and D. A. Pohlman, *Journal of Applied Physics* **107**, 103303 (2010).
- [11] N. Leoni and B. Paradkar, in *NIP & Digital Fabrication Conference*, Vol. 2009 (Society for Imaging Science and Technology, 2009) pp. 229–232.
- [12] C. Tendero, C. Tixier, P. Tristant, J. Desmaison, and P. Leprince, *Spectrochimica Acta Part B: Atomic Spectroscopy* **61**, 2 (2006).
- [13] N. S. Kopeika and N. H. Farhat, *Electron Devices, IEEE Transactions on* **22**, 534 (1975).
- [14] D. B. Graves and K. F. Jensen, *Plasma Science, IEEE Transactions on* **14**, 78 (1986).
- [15] P. Kisliuk, *Journal of Applied Physics* **30**, 51 (1959).
- [16] M. Radmilović-Radjenović, Š. Matejčik, M. Klas, and B. Radjenović, *Journal of Physics D: Applied Physics* **46**, 015302 (2013).
- [17] M. Radmilović-Radjenović and B. Radjenović, *Plasma Sources Science and Technology* **17**, 024005 (2008).
- [18] C. Spataru, D. Teillet-Billy, J. Gauyacq, P. Testé, and J. Chabrier, *Journal of Physics D: Applied Physics* **30**, 1135 (1997).
- [19] G. Ecker and K. Müller, *Journal of Applied Physics* **30**, 1466 (1959).
- [20] P. Tchertchian, C. Wagner, T. Houlahan, B. Li, D. Sievers, and J. Eden, *Contributions to Plasma Physics* **51**, 889 (2011).

- [21] P. Testé and J. Chabrierie, Journal of Physics D: Applied Physics **29**, 697 (1996).
- [22] E. L. Murphy and R. Good Jr, Physical review **102**, 1464 (1956).
- [23] X. Fang, Y. Bando, U. K. Gautam, C. Ye, and D. Golberg, Journal of Materials Chemistry **18**, 509 (2008).
- [24] M. J. Kushner, Journal of Physics D: Applied Physics **38**, 1633 (2005).
- [25] W. Boyle and P. Kisliuk, Physical Review **97**, 255 (1955).
- [26] V. Lisovskii and S. Yakovin, Technical Physics **45**, 727 (2000).
- [27] M. Klas, Š. Matejčik, B. Radjenović, and M. Radmilović-Radjenić, Physics Letters A **376**, 1048 (2012).
- [28] F. W. Strong, J. L. Skinner, and N. C. Tien, Journal of Micromechanics and Microengineering **18**, 075025 (2008).
- [29] M. Radmilović-Radjenić, B. Radjenović, M. Klas, and Š. Matejčik, Micro & Nano Letters **7**, 232 (2012).
- [30] M. Radmilović-Radjenić, J. K. Lee, F. Iza, and G. Park, Journal of physics D: applied physics **38**, 950 (2005).
- [31] M. Kulsreshath, N. Sadeghi, L. Schwaederle, T. Dufour, L. J. Overzet, P. Lefauchaux, and R. Dussart, Journal of Applied Physics **114**, 243303 (2013).
- [32] M. Klas, Š. Matejčik, B. Radjenović, and M. Radmilović-Radjenić, EPL (Europhysics Letters) **95**, 35002 (2011).
- [33] J. Eden and S. Park, Plasma physics and controlled fusion **47**, B83 (2005).
- [34] C.-H. Chen, J. A. Yeh, and P.-J. Wang, Journal of Micromechanics and Microengineering **16**, 1366 (2006).
- [35] P. Carazzetti, P. Renaud, and H. Shea, in *MOEMS-MEMS 2008 Micro and Nanofabrication* (International Society for Optics and Photonics, 2008) pp. 688404–688404.
- [36] K.-F. Chen and J. Eden, Applied Physics Letters **93**, 161501 (2008).
- [37] O. Sonoiki, “Novel designs, materials and techniques in plasma bipolar junction transistor (pbjt) fabrication and testing,” (2013), <http://hdl.handle.net/2142/45512>.
- [38] “Relaxation oscillator,” (1974), uS Patent 3,831,113.
- [39] O. Stoican, ROMANIAN JOURNAL OF PHYSICS **54**, 385 (2009).
- [40] D. Crintea, U. Czarnetzki, S. Iordanova, I. Koleva, and D. Luggenhölscher, Journal of Physics D: Applied Physics **42**, 045208 (2009).
- [41] A. A. Garamoon, A. Samir, F. F. Elakshar, A. Nosair, and E. F. Kotp, Plasma Science, IEEE Transactions on **35**, 1 (2007).
- [42] D. Mariotti, Y. Shimizu, T. Sasaki, and N. Koshizaki, Applied physics letters **89**, 201502 (2006).
- [43] J. A. Miles, *Determining Metastable Densities in an Argon Discharge Through Optical Emission Spectroscopy*, Ph.D. thesis, Wright State University (2010).
- [44] M. Schulze, A. Yanguas-Gil, A. Von Keudell, and P. Awakowicz, Journal of Physics D: Applied Physics **41**, 065206 (2008).
- [45] A. Kramida, Yu. Ralchenko, J. Reader, and NIST ASD Team, NIST Atomic Spectra Database (ver. 5.2), [Online]. Available: <http://physics.nist.gov/asd> [2014, November 25]. National Institute of Standards and Technology, Gaithersburg, MD. (2014).